

Exploring the Therapeutic Potential of Oxo berberine Compound in *Arcangelisia flava* Root Extract for Breast Cancer Treatment: Metabolite Profiling, Pharmacological Network Analysis, and *In Silico* and *In Vitro* Evaluation

Roihatul Mutiah^{1*}, Sayyida Roisatus Zahiro², Torikhotul Jauharotun Nafisah¹, Rahmi Annisa¹, Arief Suryadinata¹, Alif Firman Firdausi¹, Sukardiman Sukardiman³

Abstract

Objective: Chemotherapy treatments for breast cancer often entail side effects and drug resistance. *Arcangelisia flava* root extract (AFRE) shows potential as an anti-cancer agent, but understanding its compounds and mechanisms against breast cancer remains limited. This study aims to identify potential compounds in AFRE and shed light on its actions against breast cancer. **Methods:** Compounds in AFRE were identified via LC-MS/MS. ADMET software evaluated absorption and bioavailability. Molecular anti-cancer mechanisms were predicted using network pharmacology with tools like Cytoscape, GeneCards, Disgenet, STRING, GO, KEGG pathways, and SRplot. Interaction between oxo berberine and key breast cancer receptors was analyzed through molecular docking with PyRx Autodock Vina and Biovia Discovery Studio. Cytotoxicity was assessed using the MTT method on T47D cells, and flow cytometry evaluated the potential to inhibit the cell cycle and induce apoptosis. **Result:** A total of 16 active compounds were identified through LC-MS/MS, with oxo berberine being the most abundant at 41.43%. Importantly, it exhibited anti-cancer properties by interacting with 84 genes and affecting 13 signaling pathways related to breast cancer. We found that oxo berberine had a stronger negative binding affinity with *PI3KCA*, *TP53*, *BCL2*, *CDK1*, *EGFR*, and *MAPK14* than the native ligand, which was supported by molecular docking results. *In vitro* validation supported these results even more, showing that AFRE treatment caused more T47D cells to die (36.6%) than the control and doxorubicin, as well as more cells to gather in the G1 phase. **Conclusion:** In summary, this evidence highlights the potent anti-cancer effects of oxo berberine in AFRE against breast cancer.

Keywords: *BCL2- CDK1- EGFR- PI3KCA- T47D*

Asian Pac J Cancer Prev, 26 (4), 1313-1328

Introduction

Breast cancer is the most common cancer worldwide and a leading cause of cancer-related deaths in women. According to data from the International Agency for Research on Cancer (IARC) in 2020, there were approximately 2.3 million new cases of breast cancer and over 685,000 breast cancer-related deaths worldwide [1]. Conventional breast cancer therapies such as chemotherapy, radiotherapy, and hormone therapy have limitations in terms of efficacy and side effects [2]. Additionally, drug resistance development is a significant challenge in breast cancer treatment [3, 4]. On the other

hand, targeted therapies capable of addressing specific genetic mutations in breast cancer are not yet widely available [5]. Therefore, there is still a need for the development of new anticancer drugs to address these issues.

Arcangelisia flava (L.) Merr. is a plant belonging to the Menispermaceae family. Several studies have shown that *Arcangelisia flava* has potential as an antimalarial agent [6], antibacterial, antioxidant, immunostimulant [7, 8], and anticancer [9]. Active compounds found in *Arcangelisia flava*, such as berberine, palmatine, and jatrorrhizine, are believed to possess anticancer properties [10].

Previous research has reported that the alkaloid content

¹Department of Pharmacy, Faculty of Medicine and Health Sciences, UIN Maulana Malik Ibrahim Malang, East Java, Indonesia. ²Department of Medicine, Faculty of Medicine, Universitas Brawijaya, Malang, East Java, Indonesia. ³Department of Pharmaceutical Sciences, Faculty of Pharmacy, Universitas Airlangga, Surabaya, East Java, Indonesia. *For Correspondence: roih@farmasi.uin-malang.ac.id

in *Arcangelisia flava* root extract has the potential to reduce the survival of colorectal cancer cells WiDr [11]. Although some studies have been conducted previously, information about secondary metabolite content in *Arcangelisia flava* root extract (AFRE) is still limited, and there have been no discoveries regarding the molecular mechanisms, target genes, and pathways involved in the potential compounds from AFRE that can inhibit cancer cell growth.

Network pharmacology is a promising research approach that integrates pharmacology, molecular biology, and bioinformatics to establish network connections among effective pharmacological components, related targets, pathways, and associated diseases [12]. Thus, this approach elucidates disease progression from the perspective of systems biology, pharmacology, and biological networks. This method not only predicts the relationships between drugs and diseases from a network standpoint but also visualizes and analyzes complex biological systems [13, 14].

The main objective of this research is to profile the metabolites of compounds using LCMS/MS methods and subsequently analyze the molecular mechanisms, target genes, and potential pathways of *Arcangelisia flava* root extract (AFRE) in breast cancer treatment using network pharmacology, bioinformatics, and molecular experiments. This study aims to provide valuable insights for future pharmacological research and potential clinical therapeutic applications.

Materials and Methods

Preparation of Arcangelisia flava Roots Extract (AFRE)

The extraction of *Arcangelisia flava* roots (AFRE) was conducted using *Arcangelisia flava* roots collected under the number 074/348/102.7/2021 from an area in East Borneo, located at an altitude of 29 meters. The region had an average temperature of 26.4 degrees Celsius and an average annual rainfall of 2376 mm. The powdered roots were subjected to extraction at a ratio of 1:20 using 96% ethanol and the Ultra Assisted Extraction (UAE) method, carried out at a temperature of 25°C for 30 minutes. Subsequently, the ethanol extract was prepared for further analysis by being placed in an oven set at 40°C for 5 hours [15].

LC-MS/MS (Liquid Chromatography-Tandem Mass Spectrometry) analysis

The LC-MS/MS analysis was conducted using UPLC-MS systems equipped with a QToF analyzer and positive ESI as the ionization source. It utilized an Acquity C18 column (1.8 µm; 2.1 × 150 mm). The eluent consisted of (A) water (HPLC grade) with formic acid (Merck, Darmstadt, Germany) in a ratio of 99.9/0.1 [v/v] and (B) acetonitrile (Merck, Darmstadt, Germany) with formic acid in a ratio of 99.9/0.1 [v/v], employing a gradient elution system. The source temperature was set at 100°C, and the desolvation temperature at 350°C. A 10 mg extract was dissolved in a 10 ml volumetric flask using absolute methanol, and 5 µL of this solution was injected into the UPLC-MS system. The analysis parameters were

configured in positive ion mode, with spectra acquired across a mass range from m/z 120 to 1000. Mass Lynx version 4.1 software (Waters, Massachusetts, USA) and PubChem (<https://pubchem.ncbi.nlm.nih.gov/>) were employed for processing the chromatogram and compound identification. The confirmation of a compound's accuracy was based on MS/MS fragment matching with an inaccuracy threshold of less than 5 ppm [16].

Oral bioavailability screening

Oral Bioavailability Screening A crucial pharmacokinetic parameter, known as oral bioavailability, is employed to quantify the amount of orally administered medication that enters the bloodstream and exerts pharmacological effects (<http://www.swissadme.ch/index.php>) [17].

Identification of potential targets for breast cancer

Identification of Potential Targets for Breast Cancer One fundamental aspect of pharmaceutical research involves predicting the interactions between chemicals and specific targets. Gene targets associated with the active compounds, as determined by LC-MS/MS analysis in the *A. flava* extract, were identified using the KEGG (<https://www.genecards.org/>). Simultaneously, gene targets linked to breast cancer were explored using the DisGeNET database (<https://www.disgenet.org>). Subsequently, network pharmacology analysis was conducted using Cytoscape software version 3.9.1 to obtain an overview of the interactions between active compounds and gene targets, along with the results related to disease-gene targets [18, 19].

Construction of pharmacological networks and protein-protein interactions

The creation of pharmacological network connections involving active compounds, target genes, and diseases was performed using Cytoscape version 3.10. For further analysis, gene targets that overlapped between active compounds and diseases were selected and processed using the STRING platform version 12.0 (<https://string-db.org/>). The construction of the Protein-Protein Interaction (PPI) network included common target proteins with a minimum required interaction score of 0.400. The goal of PPI network analysis was to investigate biological activities by examining functional annotations related to Gene Ontology (GO) and Kyoto Encyclopedia of Genes and Genomes (KEGG) [20, 21].

GO Analysis and kegg pathway enrichment

The identified targets underwent Gene Ontology (GO) analysis and functional pathway enrichment, which were carried out using R. Screening criteria were set at $p = 0.05$ and $q = 0.05$ to evaluate functional enrichment results. The most significant findings in terms of cellular component (CC), molecular function (MF), and biological process (BP) were identified in the GO analysis and presented visually using R to create a bubble chart. Additionally, the top thirty KEGG pathway enrichments were utilized to generate bubble diagrams for visual representation, utilizing SRPlot (<http://www.bioinformatics.com.cn/>)

srplot) [22].

Molecular docking

In molecular docking, AutoDock Vina is utilized to obtain the best position and binding between ligands and proteins. This docking process was conducted for the oxo berberine compound with six target receptors: *PI3KCA* (PDB ID: 5DXT); *TP53* (PDB ID: 3DCY); *BCL2* (PDB ID: 2W3L); *CDK1* (PDB ID: 4Y72); *EGFR* (PDB ID: 5H5); *MAPK14* (PDB ID: 1A9U). The ligand structures were downloaded from the PubChem database, while the receptor structures were obtained from the Protein Data Bank. For initial validation, re-docking was performed between the receptors and their respective original ligands, considering an RMSD parameter that should be less than 2.0 Å. The results of the compound docking were ranked based on affinity energy values. The interactions between the ligand and receptor were visualized using Biovia Discovery Studio and PyMol 19 software [23].

Cell culture

The *T47D* breast cancer cell line was obtained from Dr. Masashi Kawaichi at the Nara Institute of Science and Technology (NAIST) in Japan. These cells were cultivated as a monolayer in high-glucose Dulbecco's Modified Eagle Medium (DMEM) (Gibco, United States) supplemented with 10% (v/v) fetal bovine serum (FBS) (Sigma, United States), 150 IU/ml penicillin, 150 µg/ml streptomycin (Gibco, United States), and 1.25 µg/ml amphotericin B (Gibco, United States). Subsequently, the cells were maintained at 37°C with a 5% CO₂ level and 100% humidity. For experiments, *T47D* cells were used when they reached approximately 80-90% confluence [24].

Cell viability assay

The proliferation of *T47D* cells was assessed using the MTT assay method. Initially, 2×10^3 *T47D* cells per well were seeded in 96-well microplates and allowed to adhere overnight. Subsequently, the cells were incubated for 24 hours with treatments, which included AFRE at concentrations ranging from 50 to 500 µM and DOX (Sigma-Aldrich, United States) at concentrations ranging from 0.01 to 10 µM. Untreated cells served as a negative control. Following treatment, 100 µL of MTT (Biovision) solution, diluted in medium (at a concentration of 0.5 mg/mL), was added to each well and incubated for 4 hours at 37°C with 5% CO₂. Next, the MTT formazan crystals were dissolved by adding a stop solution containing sodium dodecyl sulfate (SDS) with 0.01 N HCl, and then incubated overnight in the dark. Once the purple formazan solution had completely dissolved, absorbance was measured using an ELISA reader (Corona SH-1000) at a wavelength of 595 nm. Each treatment was performed in triplicate, and cytotoxic activity was determined in terms of IC₅₀, which represents the concentration required to reduce the cell population by 50% compared to untreated cells [25].

Cell Cycle Analysis

Cell cycle analysis was conducted using the

Flowcytometry method with propidium iodide (PI) staining. *T47D* cells, at a density of 2×10^5 cells per well, were cultured in six-well microplates. After treatment with AFRE at concentrations ranging from 50 to 500 µM and DOX (Sigma-Aldrich, United States) at concentrations ranging from 0.01 to 10 µM, all media were removed. The cells were then trypsinized and centrifuged at 2000 rpm for 3 minutes. The collected cells were subsequently resuspended and fixed in ethanol for 30 minutes at 4°C. The next step involved washing the cells with chilled PBS and centrifuging them at 2000 rpm for 3 minutes. The cell pellet was resuspended in a solution of PI (50 µg/ml in PBS containing 1% Triton X-100 from Merck) and DNase-free RNase A (20 µg/ml), and incubated for 30 minutes at 37°C. Finally, the cells were analyzed using Flowcytometry (FACS Calibur, BD Biosciences, United States). After electronically eliminating cell debris, red fluorescence was measured using the FL1 setting (log mode) [26].

Apoptosis assay

The apoptosis assay was conducted using the flow cytometry method, employing Annexin V-FITC/PI staining for both AFRE and DOX treatments. In brief, the collected cells were stained using the Annexin-V-FLUOS staining kit (Roche), which contained 100 ml of binding solution, 2 ml of Annexin V, and 2 ml of PI for 10 minutes at room temperature in the dark. Subsequently, these cells were measured using a flow cytometry device (FACS Calibur, BD Biosciences, United States). Fluorescence intensity was measured using the FL-1H parameter to detect FITC. Next, the percentage of apoptosis was analyzed using the Cell Quest software program (BD Bioscience) [27].

Results

The mass spectrometry analysis yielded a Total Ion Chromatogram (TIC) as shown in Figure 1, and this analysis led to the recognition of 16 compounds (Table 1) along with their respective elemental formulas. The mass spectrometry data comprises both the measured and calculated m/z, molecular formulas, error in parts per million (ppm), retention times, and MS fragmentation patterns for the identified substances.

Metabolite profiling

Based on the metabolite profile results in Figure 1, it has been found that AFRE contains 16 compounds, consisting of 11 alkaloid compounds, 3 xanthone compounds, and 1 linoleic acid compound. The dominant compound in AFRE is oxo berberine, with an area percentage of 41.43%, followed by dihydroberberine with an area percentage of 27.52%. Additionally, there are xanthone compounds, namely mangostanin with an area percentage of 4.41%, α-mangostin at 3.35%, and γ-mangostin with a percentage of 0.16% (Table 1).

The prediction of the physicochemical properties of AFRE was conducted with the aim of determining the absorption and permeability of these compounds. This prediction was based on the Lipinski's Rule of Five and

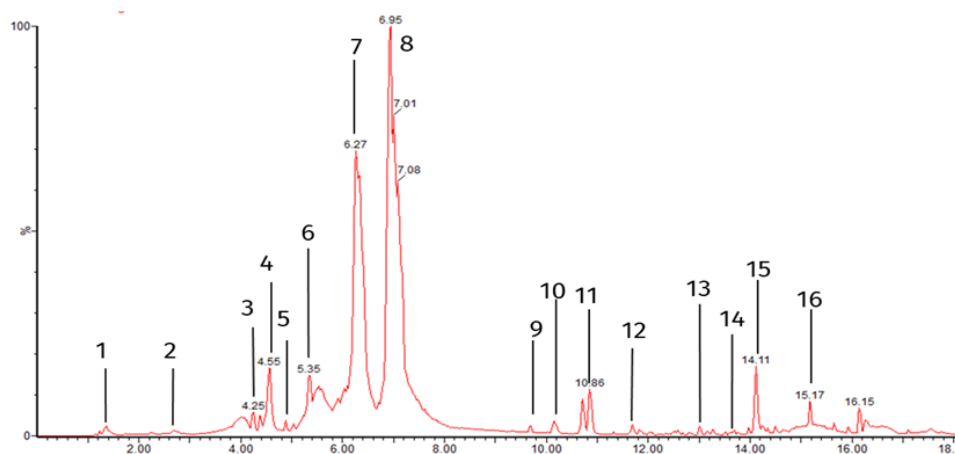


Figure 1. Chromatogram of *Arcangelisia flava* Roots Extract Using Liquid Chromatography-Tandem Mass Spectrometry (LC-MS/MS) Method. It was C18 stationary phase; the mobile phase was water/formic acid [99.9/0.1 (v/v)] and acetonitrile/formic acid 99.9/0.1 (v/v). Each chromatogram peak indicated one compound.

involved several parameters, including Molecular Weight, Log P, Hydrogen Bond Acceptors (HBA), Hydrogen Bond Donors (HBD), Torsion, and Polar Surface Area (PSA). The screening results revealed that 16 compounds met the criteria of Lipinski’s Rule of Five, indicating their potential for oral bioavailability. Table 2 presents the results of the prediction of physicochemical properties for each compound.

Potential gene targets of compounds from arcangelisia flava root extract in breast cancer treatment

In the search for potential gene targets of compounds in AFRE for breast cancer treatment using GeneCards, it was revealed that out of the 16 compounds contained in AFRE, they were associated with 336 potential gene targets. On the other hand, gene targets related to breast cancer from Disgenet reached 851 gene targets, including estrogen-positive breast cancer (CUI: C2938924) and

estrogen-negative breast cancer (CUI: C4733092). From the results of the Venn diagram analysis comparing phytochemical gene targets with disease gene targets, it was found that there were 96 potential gene targets that overlapped (Figure 2a). Subsequently, further analysis related to pharmacological networks was conducted using the Cytoscape software (Figure 2b).

The results of the pharmacological network analysis of compounds in AFRE with breast cancer target genes indicate that out of the 16 compounds present, there are 6 compounds that have the potential as potential target genes for breast cancer. These six compounds are oxo berberine with 84 target genes, alpha-Mangostin with 11 target genes, Sinomenin with 10 target genes, gamma-Mangostin with 7 target genes, Bulbocapnine with 1 target gene, and 6,7-Dimethoxy-3,4-dihydroisoquinoline with 1 target gene (Table 3).

Table 1. The Results of Metabolite Identification of *Arcangelisia flava* Roots Extract Using UPLC Qtof MS/MS Method

No	Rt	%area	Measured pass	Calculated mass	Formula	Name	Groups
1	1.344	0.62	344.1857	344.1862	C20H26NO4	6beta-Naltrexol	Alkaloid
2	2.709	0.18	192.1021	192.1025	C11H14NO2	6,7-Dimethoxy-3,4-dihydroisoquinoline	Alkaloid
3	4.002	2.58	344.1855	344.1862	C20H26NO4	6beta-Naltrexol	Alkaloid
4	4.55	3.1	344.1865	344.1862	C20H26NO4	6beta-Naltrexol	Alkaloid
5	4.881	0.02	314.175	314.1756	C19H24NO3	sinomenin	alkaloid
6	5.408	6.22	338.1386	338.1392	C20H20NO4	Dihydroberberine	alkaloid
7	6.308	27.52	338.1386	338.1392	C20H20NO4	Dihydroberberine	alkaloid
8	6.969	41.43	352.1542	352.1549	C21H22NO4	oxo berberine	alkaloid
9	9.697	0.13	326.1387	326.1392	C19H20NO4	Bulbocapnine	Alkaloid
10	10.154	0.53	322.1075	322.1079	C19H16NO4	Cepharadione B	Alkaloid
11	10.836	2.7	354.1707	354.1705	C21H24NO4	Cavidine	alkaloid
12	11.714	0.54	388.1385	388.1392	C20H20NO4	Dihydroberberine	alkaloid
13	13.008	0.18	295.227	295.2273	C18H31O3	9-OxoODE	asam linoleat
14	13.25	0.16	397.1644	397.1651	C23H25O6	g-mangostin	xanthone
15	14.112	3.35	411.1812	411.1808	C24H27O6	a-Mangostin	xanthone
16	15.188	4.41	409.1647	409.1651	C24H25O6	Mangostanin	xanthone

Table 2. The Results of the Physicochemical Prediction of 16 Compounds in *Arcangelisia flava* Root Extract

No	Compound Name	Parameters of Lipinski's five laws					Lipinski's five laws	
		BM	Log P	HBA	HBD	Torsion		
1	6beta-Naltrexol	343.423	1.3172	5	3	2	146.768	Yes
2	6,7-Dimethoxy-3,4-dihydroisoquinoline	191.23	1.6788	3	0	2	83.373	Yes
3	6beta-Naltrexol	343.423	1.3172	5	3	2	146.768	Yes
4	6beta-Naltrexol	343.423	1.3172	5	3	2	146.768	Yes
5	Sinomenin	329.396	2.0181	5	1	2	141.411	Yes
6	Dihydroberberine	337.375	3.3023	5	0	2	145.915	Yes
7	Dihydroberberine	337.375	3.3023	5	0	2	145.915	Yes
8	Oxo berberine	351.402	4.019	5	0	4	152.596	Yes
9	Bulbocapnine	325.364	2.8816	5	1	1	139.92	Yes
10	Cepharadione B	321.332	3.1693	4	0	2	137.924	Yes
11	Cavidine	339.391	3.346	5	1	1	146.285	Yes
12	Dihydroberberine	337.375	3.3023	5	0	2	145.915	Yes
13	9-OxoODE	294.435	5.0635	2	1	14	128.681	Yes
14	gamma-mangostin	396.439	4.786	6	4	4	167.208	Yes
15	alpha-Mangostin	410.466	5.089	6	3	5	173.892	Yes
16	Mangostanin	408.45	5.0589	6	2	3	173.206	Yes

Construction of Pharmacological Networks and Protein-Protein Interactions

The analysis of Protein-Protein Interactions (PPI) involving target genes in breast cancer treatment aims to identify and understand the relationships between proteins and signaling pathways that play a role in the biological processes of this disease. PPI refers to the physical or functional interactions between two or more proteins that have key roles in various cellular processes [28].

Protein-Protein Interactions (PPI) refer to the

relationships among different types of proteins in the AFRE that have roles in the biological pathways of breast cancer treatment. The results show that several compounds found in the extract, such as oxo berberine, alpha-Mangostin, Bulbocapnine, gamma-Mangostin, Sinomenin, and 6,7-Dimethoxy-3,4-dihydroisoquinoline, have the potential to interact with specific proteins involved in relevant biological processes for breast cancer treatment. These interactions can provide valuable insights into how these compounds work in inhibiting

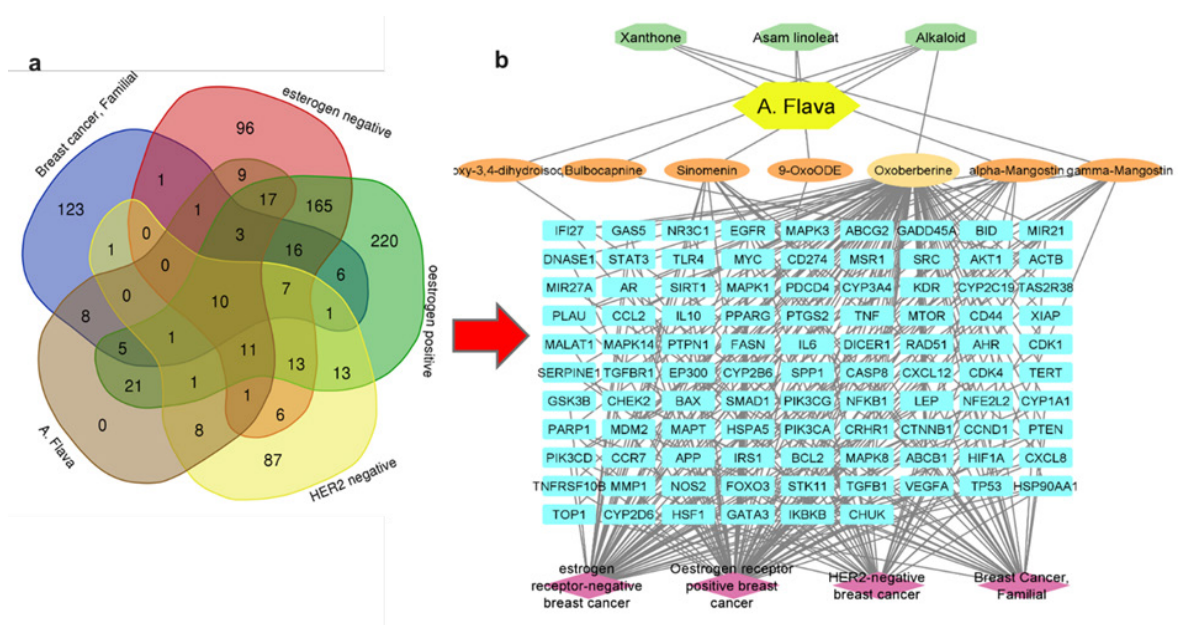


Figure 2. a) Venn diagram of gene targets for compounds in *Archengelisia flava* root extract and breast cancer disease target genes, including four types: familial breast cancer, estrogen-negative breast cancer, estrogen-positive breast cancer, and *HER2*-negative breast cancer. b) Network topology of compounds in *Archengelisia flava* root extract with target genes (Number of nodes: 111, Number of edges: 314). The yellow hexagon represents the plant's name, the blue rectangle represents a target gene, the brown ellipses represent active components, and the green hexagon represents compound categories.

Table 3. The Target Gene of the Compound in *Arcangelisia flava* Roots Extract and Relevance Score of Target Gene

Compounds	Gene Symbol	Description	Gifts	Relevance score
alpha-Mangostin	<i>PIK3CA</i>	Phosphatidylinositol-4,5-Bisphosphate 3-Kinase Catalytic Subunit Alpha	56	1.547656059
alpha-Mangostin	<i>PIK3CG</i>	Phosphatidylinositol-4,5-Bisphosphate 3-Kinase Catalytic Subunit Gamma	53	1.547656059
alpha-Mangostin	<i>PIK3CD</i>	Phosphatidylinositol-4,5-Bisphosphate 3-Kinase Catalytic Subunit Delta	57	1.547656059
alpha-Mangostin	<i>TP53</i>	Tumor Protein P53	57	1.547656059
alpha-Mangostin	<i>MAPK3</i>	Mitogen-Activated Protein Kinase 3	53	2.202917099
alpha-Mangostin	<i>MAPT</i>	Microtubule Associated Protein Tau	54	1.547656059
alpha-Mangostin	<i>MAPK1</i>	Mitogen-Activated Protein Kinase 1	57	2.202917099
alpha-Mangostin	<i>NFKB1</i>	Nuclear Factor Kappa B Subunit 1	57	2.266950607
alpha-Mangostin	<i>MDM2</i>	<i>MDM2</i> Proto-Oncogene	57	1.547656059
alpha-Mangostin	<i>PLAU</i>	Plasminogen Activator, Urokinase	55	2.266950607
alpha-Mangostin	<i>IFI27</i>	Interferon Alpha Inducible Protein 27	42	0.978802562
Bulbocapnine	<i>ACTB</i>	Actin Beta	53	0.254443914
gamma-Mangostin	<i>PIK3CA</i>	Phosphatidylinositol-4,5-Bisphosphate 3-Kinase Catalytic Subunit Alpha	56	1.416375518
gamma-Mangostin	<i>PIK3CG</i>	Phosphatidylinositol-4,5-Bisphosphate 3-Kinase Catalytic Subunit Gamma	53	1.416375518
gamma-Mangostin	<i>TP53</i>	Tumor Protein P53	57	1.416375518
gamma-Mangostin	<i>PIK3CD</i>	Phosphatidylinositol-4,5-Bisphosphate 3-Kinase Catalytic Subunit Delta	57	1.416375518
gamma-Mangostin	<i>MAPT</i>	Microtubule Associated Protein Tau	54	1.416375518
gamma-Mangostin	<i>MDM2</i>	<i>MDM2</i> Proto-Oncogene	57	1.416375518
gamma-Mangostin	<i>IFI27</i>	Interferon Alpha Inducible Protein 27	42	0.825044155
Oxo berberine	<i>PIK3CA</i>	Phosphatidylinositol-4,5-Bisphosphate 3-Kinase Catalytic Subunit Alpha	56	3.70425415
Oxo berberine	<i>AR</i>	Androgen Receptor	55	10.68938446
Oxo berberine	<i>CDK4</i>	Cyclin Dependent Kinase 4	58	7.968865871
Oxo berberine	<i>TP53</i>	Tumor Protein P53	57	8.213262558
Oxo berberine	<i>CCND1</i>	Cyclin D1	57	9.082791328
Oxo berberine	<i>AKT1</i>	AKT Serine/Threonine Kinase 1	57	4.78391552
Oxo berberine	<i>EGFR</i>	Epidermal Growth Factor Receptor	59	4.37348938
Oxo berberine	<i>BCL2</i>	<i>BCL2</i> Apoptosis Regulator	55	5.618856907
Oxo berberine	<i>MTOR</i>	Mechanistic Target Of Rapamycin Kinase	59	1.282984734
Oxo berberine	<i>IL6</i>	Interleukin 6	55	3.810469151
Oxo berberine	<i>CXCL8</i>	C-X-C Motif Chemokine Ligand 8	48	5.421284676
Oxo berberine	<i>HIF1A</i>	Hypoxia Inducible Factor 1 Subunit Alpha	52	3.05537653
Oxo berberine	<i>STAT3</i>	Signal Transducer And Activator Of Transcription 3	58	3.925266981
Oxo berberine	<i>LEP</i>	Leptin	51	3.605410576
Oxo berberine	<i>IRS1</i>	Insulin Receptor Substrate 1	51	2.580039024
Oxo berberine	<i>HSF1</i>	Heat Shock Transcription Factor 1	51	1.091430306
Oxo berberine	<i>GATA3</i>	GATA Binding Protein 3	54	2.631459713
Oxo berberine	<i>CD44</i>	CD44 Molecule (Indian Blood Group)	52	1.400488138
Oxo berberine	<i>CCL2</i>	C-C Motif Chemokine Ligand 2	53	4.824398994
Oxo berberine	<i>HSP90AA1</i>	Heat Shock Protein 90 Alpha Family Class A Member 1	55	2.435625553
Oxo berberine	<i>NR3C1</i>	Nuclear Receptor Subfamily 3 Group C Member 1	53	2.637114048
Oxo berberine	<i>ACTB</i>	Actin Beta	53	0.712083817
Oxo berberine	<i>PTEN</i>	Phosphatase And Tensin Homolog	55	3.058615923
Oxo berberine	<i>PDCD4</i>	Programmed Cell Death 4	47	2.115552425
Oxo berberine	<i>SRC</i>	<i>SRC</i> Proto-Oncogene, Non-Receptor Tyrosine Kinase	55	3.561684608
Oxo berberine	<i>CXCL12</i>	C-X-C Motif Chemokine Ligand 12	49	0.60043323
Oxo berberine	<i>MIR21</i>	MicroRNA 21	25	3.04287076
Oxo berberine	<i>MAPT</i>	Microtubule Associated Protein Tau	54	5.517550945
Oxo berberine	<i>CHEK2</i>	Checkpoint Kinase 2	58	0.984916329
Oxo berberine	<i>MYC</i>	<i>MYC</i> Proto-Oncogene, BHLH Transcription Factor	56	2.953542233
Oxo berberine	<i>CDK1</i>	Cyclin Dependent Kinase 1	52	8.114894867
Oxo berberine	<i>NOS2</i>	Nitric Oxide Synthase 2	53	3.5732584

Table 3. Continued

Compounds	Gene Symbol	Description	Gifts	Relevance score
Oxo berberine	<i>VEGFA</i>	Vascular Endothelial Growth Factor A	53	3.105199099
Oxo berberine	<i>MAPK14</i>	Mitogen-Activated Protein Kinase 14	54	5.239643574
Oxo berberine	<i>NFE2L2</i>	<i>NFE2</i> Like BZIP Transcription Factor 2	52	7.840360165
Oxo berberine	<i>PPARG</i>	Peroxisome Proliferator Activated Receptor Gamma	57	5.087024689
Oxo berberine	<i>BAX</i>	<i>BCL2</i> Associated X, Apoptosis Regulator	55	4.199271202
Oxo berberine	<i>RAD51</i>	<i>RAD51</i> Recombinase	54	2.876240969
Oxo berberine	<i>TAS2R38</i>	<i>Taste 2</i> Receptor Member 38	40	1.9029212
Oxo berberine	<i>PTPN1</i>	Protein Tyrosine Phosphatase Non-Receptor Type 1	54	2.821006298
Oxo berberine	<i>TNFRSF10B</i>	<i>TNF</i> Receptor Superfamily Member 10b	54	1.907050133
Oxo berberine	<i>GAS5</i>	Growth Arrest Specific 5	25	2.371072769
Oxo berberine	<i>TGFB1</i>	Transforming Growth Factor Beta Receptor 1	58	1.107806683
Oxo berberine	<i>TNF</i>	Tumor Necrosis Factor	55	5.727074623
Oxo berberine	<i>DNASE1</i>	Deoxyribonuclease 1	48	1.667191148
Oxo berberine	<i>PARP1</i>	Poly(ADP-Ribose) Polymerase 1	54	5.788198471
Oxo berberine	<i>CTNNB1</i>	Catenin Beta 1	57	2.516744614
Oxo berberine	<i>FASN</i>	Fatty Acid Synthase	53	3.506016731
Oxo berberine	<i>CRHR1</i>	Corticotropin Releasing Hormone Receptor 1	47	0.367453635
Oxo berberine	<i>CHUK</i>	Component Of Inhibitor Of Nuclear Factor Kappa B Kinase Complex	54	6.894852161
Oxo berberine	<i>MALAT1</i>	Metastasis Associated Lung Adenocarcinoma Transcript 1	25	0.480420917
Oxo berberine	<i>KDR</i>	Kinase Insert Domain Receptor	57	2.76473093
Oxo berberine	<i>MMP1</i>	Matrix Metalloproteinase 1	54	2.904874325
Oxo berberine	<i>NFKB1</i>	Nuclear Factor Kappa B Subunit 1	57	3.838563442
Oxo berberine	<i>SMAD1</i>	<i>SMAD</i> Family Member 1	48	0.367453635
Oxo berberine	<i>MDM2</i>	<i>MDM2</i> Proto-Oncogene	57	1.978947997
Oxo berberine	<i>SIRT1</i>	Sirtuin 1	53	2.730642796
Oxo berberine	<i>APP</i>	Amyloid Beta Precursor Protein	54	1.12212491
Oxo berberine	<i>IKBKB</i>	Inhibitor Of Nuclear Factor Kappa B Kinase Subunit Beta	58	2.83296895
Oxo berberine	<i>HSPA5</i>	Heat Shock Protein Family A (Hsp70) Member 5	53	2.109571218
Oxo berberine	<i>AHR</i>	Aryl Hydrocarbon Receptor	51	4.636149406
Oxo berberine	<i>TERT</i>	Telomerase Reverse Transcriptase	55	4.864749432
Oxo berberine	<i>PTGS2</i>	Prostaglandin-Endoperoxide Synthase 2	53	5.606129646
Oxo berberine	<i>ABCG2</i>	ATP Binding Cassette Subfamily G Member 2 (Junior Blood Group)	53	4.269975662
Oxo berberine	<i>TLR4</i>	Toll Like Receptor 4	55	1.721343279
Oxo berberine	<i>SPP1</i>	Secreted Phosphoprotein 1	50	2.262959957
Oxo berberine	<i>EP300</i>	E1A Binding Protein P300	56	2.057775974
Oxo berberine	<i>GSK3B</i>	Glycogen Synthase Kinase 3 Beta	54	1.661813736
Oxo berberine	<i>STK11</i>	Serine/Threonine Kinase 11	54	2.752609015
Oxo berberine	<i>GADD45A</i>	Growth Arrest And DNA Damage Inducible Alpha	47	2.353597879
Oxo berberine	<i>TGFBRI</i>	Transforming Growth Factor Beta Receptor 1	58	1.107806683
Oxo berberine	<i>CASP8</i>	Caspase 8	56	9.029740334
Oxo berberine	<i>DICER1</i>	<i>Dicer 1</i> , Ribonuclease III	52	1.085201025
Oxo berberine	<i>MSR1</i>	Macrophage Scavenger Receptor 1	49	2.372523069
Oxo berberine	<i>ABCB1</i>	ATP Binding Cassette Subfamily B Member 1	55	7.521132469
Oxo berberine	<i>MIR27A</i>	MicroRNA 27a	24	1.121391535
Oxo berberine	<i>MAPK8</i>	Mitogen-Activated Protein Kinase 8	53	4.175397396
Oxo berberine	<i>PLAU</i>	Plasminogen Activator, Urokinase	55	3.448729515
Oxo berberine	<i>SERPINE1</i>	Serpin Family E Member 1	54	2.853304148
Oxo berberine	<i>TOP1</i>	DNA Topoisomerase I	53	3.203369617
Oxo berberine	<i>BID</i>	BH3 Interacting Domain Death Agonist	50	3.171581268
Oxo berberine	<i>FOXO3</i>	Forkhead Box O3	51	1.54453373
Oxo berberine	<i>XIAP</i>	X-Linked Inhibitor Of Apoptosis	55	1.254233479

Table 3. Continued

Compounds	Gene Symbol	Description	Gifts	Relevance score
Sinomenin	<i>CXCL8</i>	C-X-C Motif Chemokine Ligand 8	48	1.477083921
Sinomenin	<i>GATA3</i>	GATA Binding Protein 3	54	2.160260439
Sinomenin	<i>TNF</i>	Tumor Necrosis Factor	55	1.617112041
Sinomenin	<i>NFKB1</i>	Nuclear Factor Kappa B Subunit 1	57	0.906536996
Sinomenin	<i>PTGS2</i>	Prostaglandin-Endoperoxide Synthase 2	53	3.387003183
Sinomenin	<i>CD274</i>	CD274 Molecule	49	1.527534842
Sinomenin	<i>ABCB1</i>	ATP Binding Cassette Subfamily B Member 1	55	0.719805062
Sinomenin	<i>MDM2</i>	<i>MDM2</i> Proto-Oncogene	57	1.184889197
Sinomenin	<i>CCR7</i>	C-C Motif Chemokine Receptor 7	48	1.421279669
Sinomenin	<i>IL10</i>	Interleukin 10	52	1.527534842
6,7-Dimethoxy-3,4-dihydroisoquinoline	<i>ABCB1</i>	ATP Binding Cassette Subfamily B Member 1	55	3.635909796

or influencing the development of breast cancer, which, in turn, can aid in the development of more effective therapies for this disease (Figure 3).

GO (Gene Ontology) Analysis and KEGG (Kyoto Encyclopedia of Genes and Genomes) pathway enrichment

The results of gene ontology analysis indicate that compounds found in AFRE, particularly oxo berberine, α -mangostin, and γ -mangostin, have an impact on biological processes, molecular functions, and cellular components. In the enrichment bubble plot, it is found that there are ten highly potential biological processes, with peptidyl serine modification and epithelial cell proliferation being the most significant, involving a total of 29 genes. This is followed by the regulation of the apoptosis signaling pathway, peptidyl serine phosphorylation, and various other biological processes involving approximately 23-28 genes (Figure 4a). Additionally, oxo berberine, α -mangostin, and γ -mangostin also influence molecular

functions, with the top 10 molecular functions being represented by activities such as protein serine/threonine kinase activity, DNA binding, transcription factor binding, ubiquitin protein binding, and others (Figure 4b). As for cellular components, the highest potential is observed in raft membranes, microdomain membranes, and other membrane regions (Figure 4c).

In the KEGG enrichment analysis, it was discovered that there are 29 pathways with significant potential in breast cancer treatment influenced by oxo berberine, α -mangostin, and γ -mangostin compounds (Figure 5). Some of these pathways include the PI3K-Akt signaling pathway (hsa0451), *p53* signaling pathway (hsa04115), apoptosis (hsa04210), cell cycle (hsa4110), resistance to *EGFR* tyrosine kinase inhibitors (hsa01521), and the *MAPK* signaling pathway (hsa04010) (Table 4). All of these pathways are predicted to have interconnections and exert influence on the biological processes involved in breast cancer treatment.

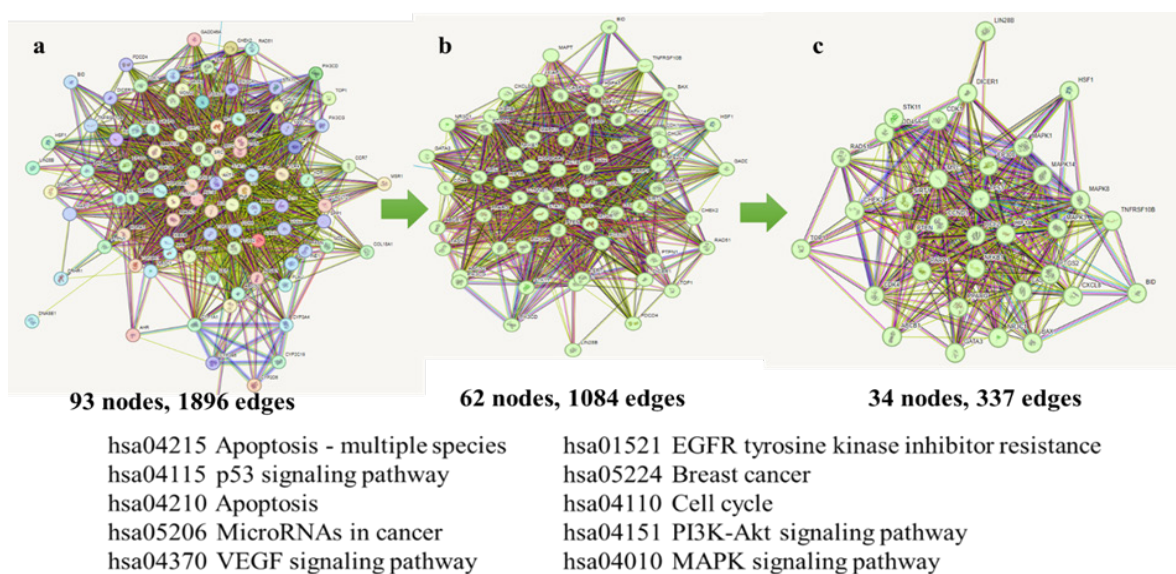


Figure 3. Protein-Protein Interaction (PPI) of Compounds in *Arcangelisia flava* Root Extract Involved in the Biological Pathway of Breast Cancer Treatment. The compounds include oxo berberine, α -mangostin, Bulbocapnine, γ -mangostin, Sinomenin, and 6,7-Dimethoxy-3,4-dihydroisoquinoline. a) PPI interactions involving all target genes of the compounds, with 93 gene targets (nodes) and 1896 interactions (edges). b) PPI interactions resulting from clustering PPI A, showing 62 gene targets (nodes) and 1084 interactions (edges). c) PPI interactions resulting from clustering PPI B, yielding 34 gene targets (nodes) and 337 interactions (edges).

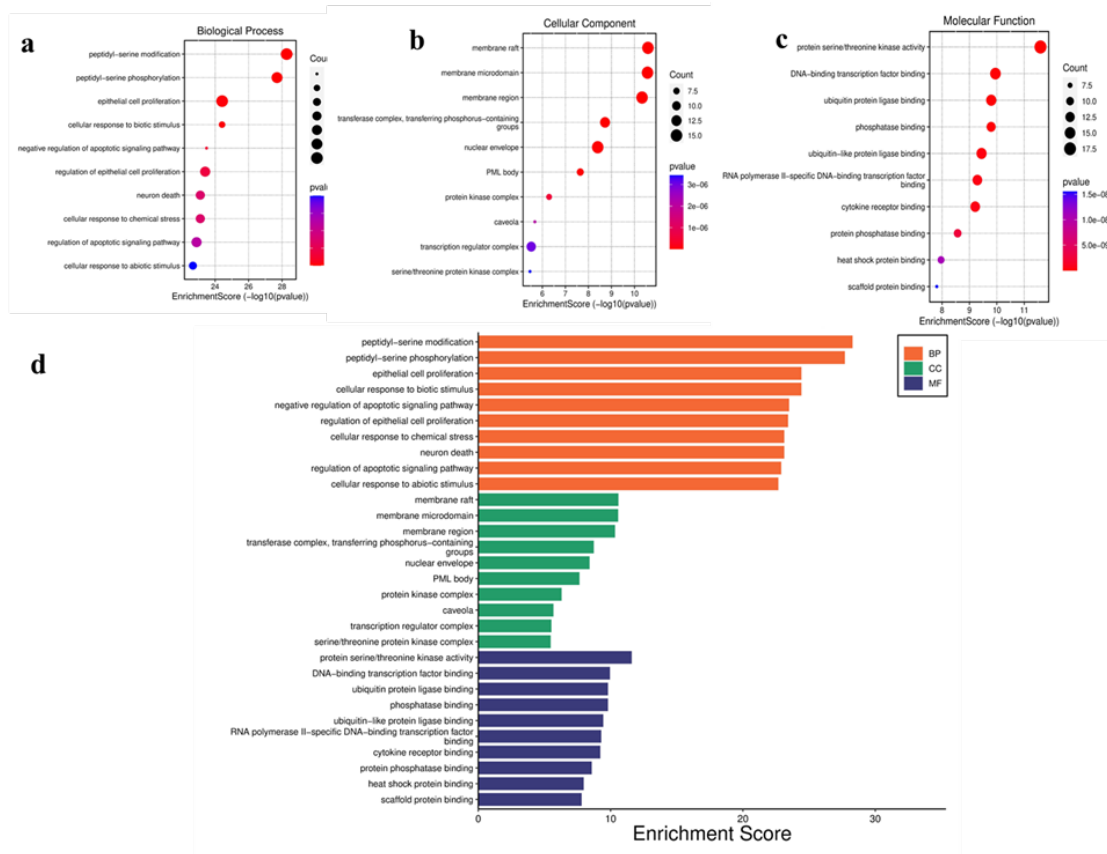


Figure 4. Gene Ontology and KEGG Pathway Enrichment Analysis; a) Bubble chart depicting the top 10 highly potential enriched biological processes; b) Bubble chart illustrating the top 10 highly potential molecular functions; c) Bubble chart displaying the top 10 cellular components. d) GO enrichment bar chart for Biological Processes, Cellular Components, and Molecular Functions.

Table 4. Signaling Pathways with KEGG Enrichment Target Numbers Equal to or Greater than 10.

ID	Pathway	Number Of Genes	Genes
hsa04115	<i>p53</i> signaling pathway	11	<i>CCNB1, CDK2, BCL2, CASP3, CHEK1, IGFBP3, MDM2, BAX, CCNB2, TP53</i>
hsa04210	Apoptosis	12	<i>TRAIL-R, TNFα, CASP8, BID, IAPX1A, actin, PARP, Bax, BCL2, Akt/PKB, ERK1/2, IKK, NFκb, P53, GADD45, TRAILR2</i>
hsa05206	MicroRNAs in cancer	12	<i>PDGFRB, ABCB1, HDAC1, PRKCA, CDC25C, PTGS2, SIRT1, MMP9, CDC25A, EGFR, MTOR, CDC25B, PIK3CA, CASP3, ERBB2, MDM2, PIMI, BCL2, MAPK1, MCL1</i>
hsa01521	<i>EGFR</i> tyrosine kinase inhibitor resistance	15	<i>EGFR, BGFR, SRC, PI3K, PTEN, PKB/AKT, mTOR, GSK3, FOXO3A, VGEF, EGFRV8, IL6, BCL2, BAX, ERK</i>
hsa04110	Cell cycle	12	<i>GSK3B, cMYC, TGFB, MDM2, P53, P300, GADD45, CHK1, 2, CYCD, CDK4, CDK6, CDK1</i>
hsa04151	<i>PI3K-Akt</i> signaling pathway	10	<i>CSF1R, GSK3B, RELA, EGFR, PIK3CG, IGF1R, RXRA, ERBB2, KDR, MAPK1, ITGA, JAK2, MCL1, PDGFRB, NTRK1, HSP90AA1, BAD, PRKCA, MTOR, PIK3CA, CDK2, BCL2, MDM2, FGFR1, BCL2L1</i>
hsa04010	<i>MAPK</i> signaling pathway	21	<i>PDGFRB, NTRK1, CSF1R, JUN, BRAF, PRKCA, MAPK14, EGFR, RELA, CDC25B, IGF1R, MAPK11, PPM1B, MAPK8, CASP3, ERBB2, KDR, MAPK1, MAP3K8, FGFR1, MAP3K5</i>
hsa04657	<i>IL-17</i> signaling pathway	13	<i>JUN, MMP1, MAPK14, PTGS2, HSP90AA1, GSK3B, MMP9, RELA, MAPK11, MAPK8, MMP13, CASP3, dan MAPK1.</i>
hsa04630	JAK-STAT signaling pathway	10	<i>PDGFRB, PIK3CA, BCL2, PIMI, PTPN6, JAK2, EGFR, PTPN2, MTOR, BCL2L1, MCL1</i>
hsa04152	AMPK signaling pathway	10	<i>CCNA2, PFKFB3, PIK3CA, FASN, PPARG, SIRT1, FBP1, CFTR, MTOR, IGF1R</i>
hsa04915	Estrogen signaling pathway	10	<i>HSP90AA1, JUN, PIK3CA, SRC, MMP2, BCL2, MAPK1, ESRI, MMP9, EGFR</i>
hsa04012	ErbB signaling pathway	12	<i>GSK3B, JUN, MAPK8, PIK3CA, SRC, BAD, ERBB2, MAPK1, BRAF, PRKCA, EGFR, MTOR</i>
hsa04014	Ras signaling pathway	14	<i>PDGFRB, NTRK1, CSF1R, BAD, PRKCA, EGFR, RELA, IGF1R, MAPK8, PIK3CA, KDR, MAPK1, FGFR1, BCL2L1</i>

The analysis of potential pathways indicates that compounds in *Arcangelisia flava* root extract (AFRE), particularly oxo berberine, α -mangostin, and γ -mangostin, exert significant influence on the regulation of several signaling pathways involved in biological processes. Among the 29 pathways considered (Figure 5), 13 of them involve more than 10 target genes within each pathway affected by these compounds. This suggests the complexity of interactions between the active components of AFRE and the signaling pathways within the cell.

Molecular docking

The results of molecular docking revealed that oxo berberine exhibited strong affinities towards six receptors, namely *PI3KCA*, *TP53*, *BCL2*, *CDK1*, *EGFR*, and *MAPK14*. The highest affinity was observed in the interaction with the *CDK1* receptor, followed by *EGFR*, *PI3KCA*, *TP53*, *BCL2*, and *MAPK14* (Figure 6). Higher affinity indicates a more stable binding between the drug and the receptor. In the context of oxo berberine's interaction with receptors in this molecular docking study, oxo berberine revealed its best activity in regulating apoptosis and cell cycle pathways related to breast cancer.

The in vitro cytotoxicity test

In our study, after analyzing the potential of anticancer compounds through pharmacological network analysis and subsequent *in silico* testing, we conducted in vitro

validation through cytotoxicity testing on breast cancer cell lines. Additionally, we also investigated signaling pathways through apoptosis and cell cycle assays. The cytotoxicity test results revealed that the AFRE exhibited moderate anticancer activity against *T47D* cells (Figure 7).

In this study, it was found that in the survival percentage graph (Figure 7), the IC_{50} value of AFRE on *T47D* cells is 400.535 $\mu\text{g/mL}$. Based on the level of anti-cancer activity, the IC_{50} value obtained indicates a classification of cytotoxic activity that is moderately active against *T47D* cells.

Apoptosis induction and cell cycle arrest

As additional evidence from pharmacological network analysis and *in silico* results indicating the involvement of AFRE compounds in apoptosis and cell cycle regulation in breast cancer cells, we conducted apoptosis and cell cycle assays. Our research results in the apoptosis assay show that AFRE compounds are reasonably effective in inducing apoptosis in breast cancer cells, with a total of 5.6% undergoing apoptosis and 26% undergoing necrosis. These results demonstrate better induction compared to untreated controls and doxorubicin-treated cells (Figure 8). Statistical analysis of the number of cells undergoing apoptosis did not show a significant difference between the AFRE-treated group and the untreated control group ($p > 0.001$). However, there was a significant difference in the number of cells undergoing necrosis ($p < 0.0001$).

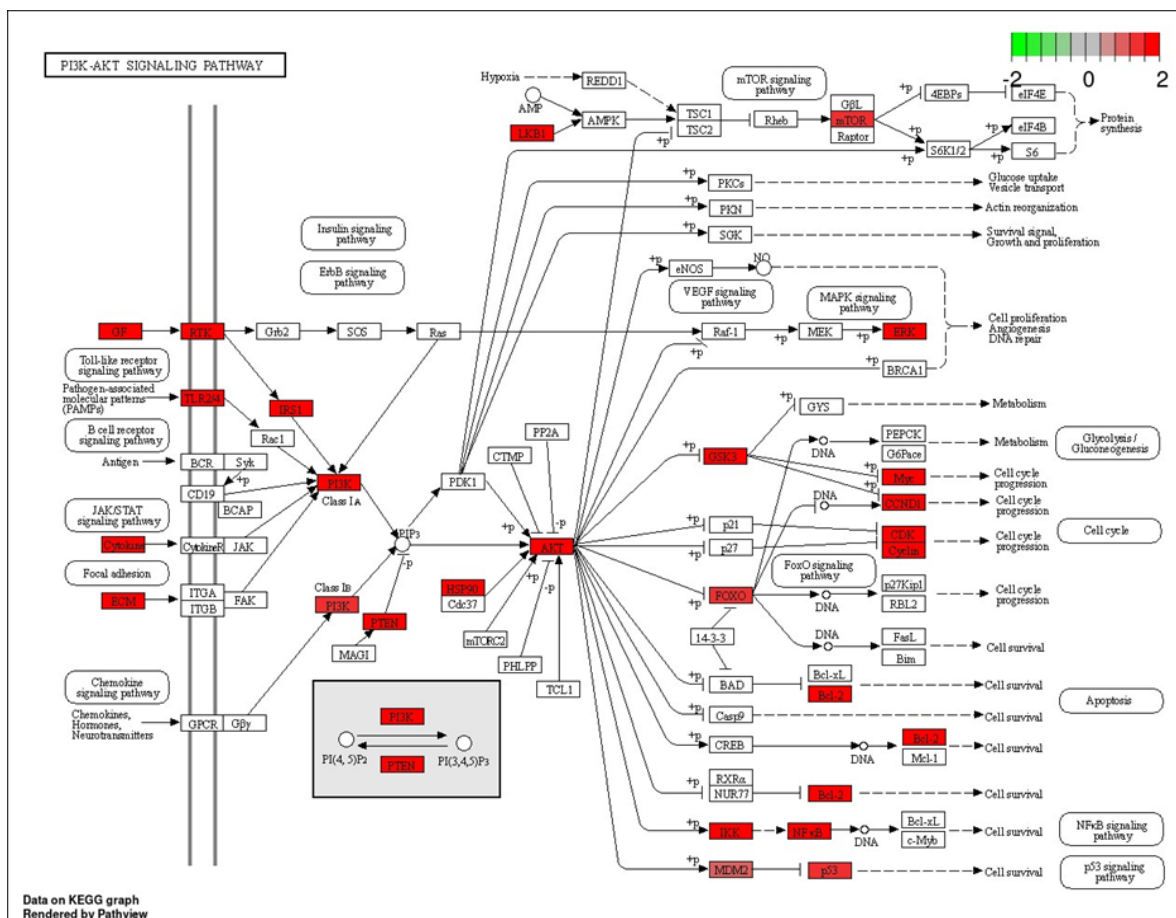


Figure 5. hsa04151 PI3K-Akt Signaling Pathway Involving 29 Potential Target Genes (highlighted in red) in Breast cancer treatment with *Archangelisia flava* root extract.

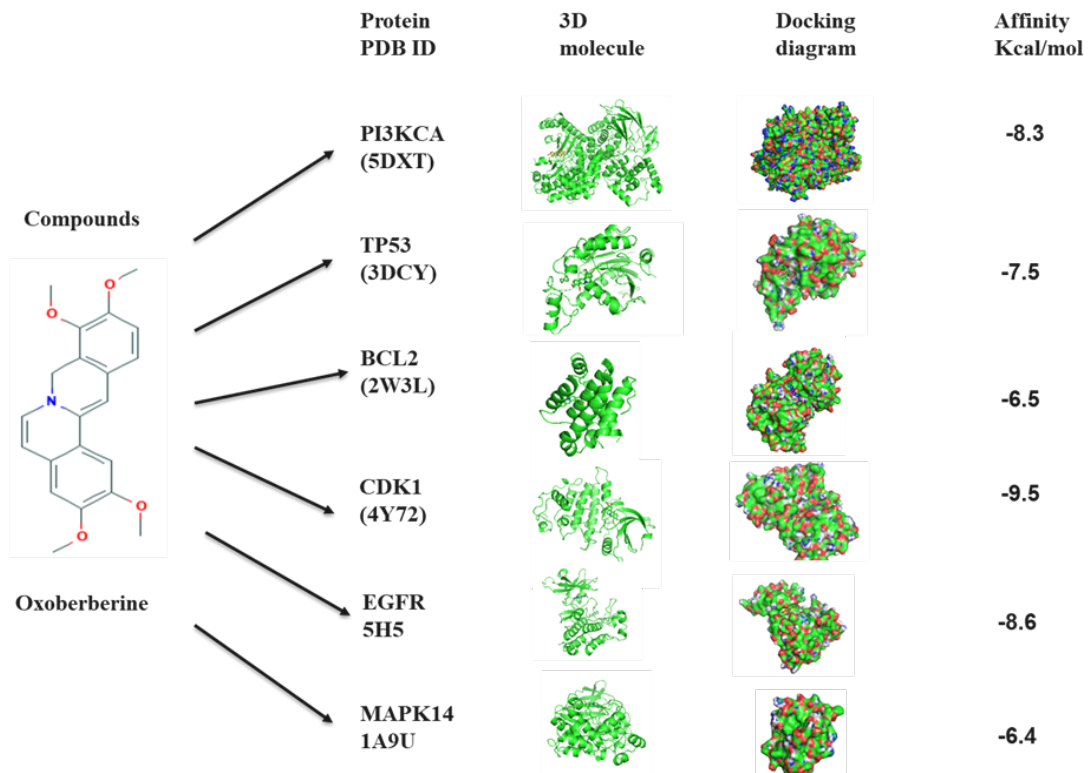


Figure 6. Docking Molekuler Senyawa Oxo Berberine Dengan Protein Target Potensial Pada Treatment Breast Cancer

In addition to inducing cell death, drug targeting is also aimed at regulating the cell cycle. Flow cytometry was used to determine the cell cycle distribution after treatment. *T47D* cells were treated with 10 nM Doxorubicin and AFRE IC_{50} for 24 hours. The results in Figure 2C, D indicate differences in the cell cycle distribution between the AFRE-treated group and the untreated control and doxorubicin-treated groups. AFRE treatment resulted in the accumulation of cancer cells in the G1 phase, preventing them from entering the next cell cycle.

Discussion

One of the failures in chemotherapy treatment is the high occurrence of undesirable side effects and the increased drug resistance [29]. The use of traditional

medicine can serve as an alternative to address these issues [30]. *Arcangelisia flava* is a traditional Indonesian medicinal plant widely utilized for its anticancer properties. Previous research has never reported which compounds are contained in *Arcangelisia flava* (AFRE) and the potential of these compounds in inhibiting the proliferation of cancer cells, particularly breast cancer. Furthermore, the gene targets and pathways involved in the biological process of cancer treatment have also not been reported.

This study aims to identify the metabolite profile of compounds using LCMS/MS methods and further explore the molecular mechanisms, gene targets, and potential pathways involved in the breast cancer treatment effect of *Arcangelisia flava* root extract (AFRE).

In the LCMSMS analysis, it has been revealed that AFRE contains 16 active compounds, and approximately



Figure 7. Viability of T47D Cells after Treatment with Doxorubicin (A) and Arcangelisia Flava Root Extract (B). For 24 hours, T47D cells were treated with various concentrations and cell viability was evaluated using the MTT (3-(4,5-dimethylthiazol-2-yl)-2,5-diphenyltetrazolium bromide) assay. The cell viability profile is presented as the mean \pm standard deviation (SD) of three independent experiments.

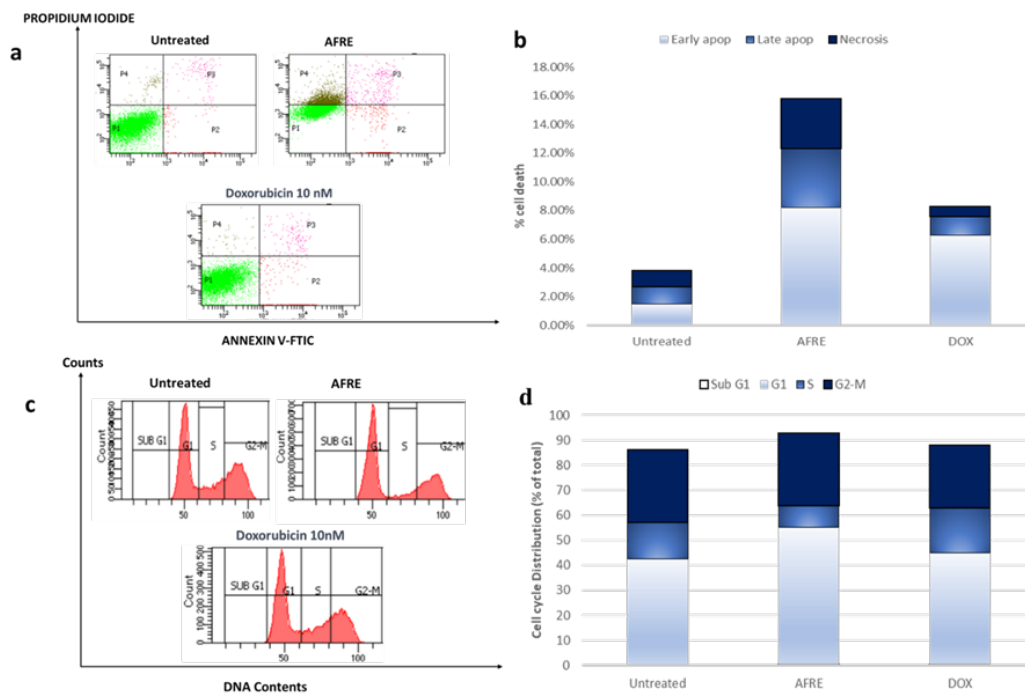


Figure 8. Apoptosis Induction and Cell Cycle Distribution by *Arcangelisia Flava* Root Extract in *T47D* Breast Cancer Cells. Cells were exposed to *Arcangelisia Flava* Root Extract for 24 hours. Cell death percentage (a, b) and cell distribution in each phase (c, d) were measured using flow cytometry after staining with Annexin V-FITC (fluorescein isothiocyanate) and PI (propidium iodide), respectively. The lines represent the mean \pm standard deviation (SD) values from three independent experiments. * $p < 0.001$ (post-hoc LSD test between each group) considered statistically significant

75% of the identified compounds belong to the alkaloid group. In this study, it was found that the compound oxo berberine has the highest concentration in AFRE extract, reaching approximately 41.43%. Oxo berberine is a quaternary alkaloid believed to be the main compound responsible for the pharmacological effects of AFRE. This is in line with previous research that has reported that *Arcangelisia flava* contains the alkaloid berberine [10].

In the pharmacological network analysis, it has been determined that oxo berberine has a substantial number of target genes associated with breast cancer, totaling 84 target genes. Our findings also revealed that in protein-protein interaction (PPI) and gene ontology analysis, compounds in AFRE, especially oxo berberine, are involved in several potential pathways relevant to breast cancer treatment. These pathways include the PI3K-Akt pathway (hsa0451), *p53* signaling pathway (hsa04115), apoptosis (hsa04210), cell cycle (hsa4110), resistance to *EGFR* tyrosine kinase inhibitors (hsa01521), and the *MAPK* signaling pathway (hsa04010) (as listed in Table 4). The results of this study are consistent with previous research, in which compounds structurally similar to berberine have been reported to downregulate the *PI3K-Akt* pathway [31], induce *P53*-dependent cell cycle and apoptosis [32], inhibit *EGFR* [33], and suppress *MAPK* [34].

In the GO and KEGG enrichment analysis conducted, oxo berberine was identified as a component playing a crucial role in up to 13 potential pathways involved in breast cancer healing. Among these numerous pathways, oxo berberine notably stands out in two major pathways,

namely the apoptosis pathway and the cell cycle pathway. In the apoptosis pathway, 12 genes are involved, including *TRAIL-R*, *TNF α* , *CASP8*, *BID*, *IAPXIAP*, *actin*, *PARP*, *Bax*, *BCL2*, *Akt/PKB*, *ERK1/2*, *IKK*, *NF κ B*, *P53*, *GADD45*, and *TRAILR2*. Additionally, in the cell cycle pathway, 12 genes also play a role, including *GSK3B*, *cMYC*, *TGFB*, *MDM2*, *P53*, *P300*, *GADD45*, *CHK1*, *CHK2*, *CYCD*, *CDK4,6*, and *CDK1*. These findings indicate the potential role of oxo berberine in regulating the breast cancer healing process through its influence on key pathways in cell regulation.

Oxo berberine can affect the apoptosis pathway in breast cancer cells, particularly through its impact on the genes *BCL2* (B-cell lymphoma 2), *TRAIL* (Tumor Necrosis Factor-Related Apoptosis-Inducing Ligand), *CASP8* (Caspase 8), and *CASP3/7* (Caspase 3/7). Oxo berberine is predicted to reduce the expression of *BCL2*, resulting in a decrease in *Bcl-2* protein levels. Thus, this influence can induce apoptosis by weakening the protective mechanism provided by *Bcl-2*. *In silico* validation results through molecular docking between oxo berberine and the *BCL2* protein (PDB ID: 2W3L) show that oxo berberine has excellent affinity with energy generated almost similar to the active ligand. This means that oxo berberine can form a stable bond with the *BCL2* receptor (PDB ID: 2W3L). The results of this study are supported by previous research that reported that berberine compounds, which have a core alkaloid structure similar to oxo berberine, are also known to downregulate the expression of *BCL2*, leading to apoptosis induction [35]. *TRAIL* (Tumor Necrosis Factor-Related Apoptosis-Inducing Ligand) is a protein that can trigger the apoptosis pathway in cancer cells

[36]. Oxo berberine can increase the expression of the *TRAIL* gene or stimulate *TRAIL* activity. This implies that oxo berberine can enhance the production of *TRAIL* by breast cancer cells or make these cells more responsive to existing *TRAIL*. *TRAIL* then functions as a “death signal” that directs cancer cells to initiate the apoptosis process. CASP8 (Caspase 8) is a key enzyme in the extrinsic apoptosis pathway [37]. Oxo berberine can influence the activity of CASP8 by activating it. CASP8 typically plays a role in initiating a cascade of reactions leading to CASP3/7 activation, which, in turn, triggers the cleavage of crucial proteins for cancer cells [37]. The activation of CASP8 by oxo berberine is a crucial step in the apoptosis process induced by this compound.

Overall, based on the analysis of Gene Ontology and KEGG, oxo berberine is predicted to influence the apoptosis pathway in breast cancer cells by inhibiting *BCL2*, increasing *TRAIL* production, activating CASP8, and ultimately inducing CASP3/7 activation. This leads to the controlled apoptosis-mediated death of breast cancer cells. *In vitro* test results show that AFRE is capable of inducing apoptosis with a higher percentage of apoptosis compared to the control and doxorubicin.

In the enrichment analysis of GO and KEGG in this study, it is also indicated that Oxo berberine has the potential to influence the cell cycle pathway in breast cancer treatment, including its effects on target genes such as *GSK3B*, *CDK4*, *CDK6*, *CDK1* (Cyclin A), and *CDK1* (Cyclin B). Oxo berberine’s mechanism of action in breast cancer treatment through its impact on the cell cycle pathway involves the regulation of the expression of target genes or the activity of enzymes involved in cell cycle regulation. By inhibiting the activity or regulating the expression of these genes, oxo berberine can help halt the growth of breast cancer cells and trigger apoptosis. *GSK3B* is an enzyme that plays a crucial role in cell cycle regulation, particularly in controlling the stability of proteins that regulate the cell cycle [38]. Oxo berberine can influence the activity of *GSK3B*, which in turn affects the stability of specific cell cycle proteins. In breast cancer treatment, inhibiting the activity of *GSK3B* can result in increased stability of proteins that inhibit the growth of cancer cells. *CDK4* and *CDK6* are kinases that regulate the G1 (Gap 1) phase in the cell cycle [39]. Oxo berberine can influence the expression or activity of *CDK4* and *CDK6*, which can inhibit the ability of breast cancer cells to progress to the next phase of the cell cycle. This can help in halting the growth of cancer cells. *CDK1*, also known as cyclin-dependent kinase 1, plays a crucial role in regulating the transition of cells from the G2 phase to the M phase (mitosis) in the cell cycle [40]. KEGG analysis results have revealed that Oxo berberine can affect the expression or activity of *CDK1* and its complex with cyclin A and cyclin B. In breast cancer treatment, inhibiting or modulating *CDK1* can disrupt the ability of cancer cells to undergo mitosis and proliferate.

In molecular docking studies, it was found that oxo berberine has the highest affinity for *CDK1* (PDB ID: 4Y72) compared to other receptors. *In vitro* testing using extracts from *Arcangelisia flava* on *T47D* cells also indicated that these cells accumulate in the G1 phase.

This leads to the inhibition of the cancer cells’ ability to progress to the next phase in the cell cycle, ultimately resulting in the cessation of cancer cell growth.

In the Gene Ontology and KEGG pathway enrichment analysis, this study also revealed significant findings regarding the influence of oxo berberine on the PI3K-Akt pathway, particularly in the context of specific gene activation. The results of this study indicate that oxo berberine interacts with several key genes in the *PI3K-Akt* pathway, such as *PIK3CA*, *CDK4*, *EGFR*, *BCL2*, *MDM2*, *MAPK1*, *GSK3B*, *HSPA5*, *Myc*, and *NFE2L2*.

The PI3K-Akt pathway plays a central role in regulating various crucial aspects of cell life, including cell growth regulation, proliferation, and involvement in many crucial cellular processes. Genes involved in this pathway have a major role in controlling the cell cycle, regulating apoptosis, and responding to external growth signals, as documented in scientific literature [41, 42].

Furthermore, it has been found that oxo berberine has the ability to modulate the activity of the *PI3K-Akt* pathway by altering the expression of involved genes. Specifically, oxo berberine has an inhibitory effect on the *CDK4* gene, which plays a crucial role in controlling the cell cycle, and it enhances the *BCL2* gene, which functions as an apoptosis inhibitor. This data is reinforced by *in silico* validation results through molecular docking, which showed significant affinity of oxo berberine compound with the *CDK4* and *BCL2* receptors.

In addition to its impact on the PI3K-Akt pathway, this study also reveals that oxo berberine has effects on other genes related to the cellular response to oxidative stress and regulates the transcription factor *NFE2L2*. These findings indicate the potential of oxo berberine in managing the cell’s response to oxidative damage and activating cellular protection mechanisms.

In the GO and KEGG enrichment analysis, this research also reveals that oxo berberine affects the *p53* signaling pathway, with involved genes being *BCL2*, *CASP3*, *TP53*, *BAX*, and *MDM2*. The *p53* signaling pathway plays a central role in maintaining genomic stability and regulating the cell’s response to DNA damage and other stress factors. Oxo berberine can influence the expression of the *Bcl2* gene in the *p53* signaling pathway. *Bcl2* is a gene that regulates the balance between cell survival and apoptosis [43]. The reduction in *Bcl2* expression induced by oxo berberine can lead to an increased tendency of cells to undergo apoptosis, which is crucial in eliminating cells with severe damage or significant DNA mutations. Oxo berberine also has an impact on the expression of Caspase-3, a key enzyme in the apoptosis pathway. Activation of Caspase-3 is a critical step in the cell death process. Therefore, the effect of oxo berberine on Caspase-3 can accelerate or enhance the apoptosis pathway in response to cellular stress or DNA damage.

Oxo berberine can also affect the expression of the Bax gene in the *p53* signaling pathway. Bax is a member of the *Bcl2* family that facilitates the release of cytochrome c from mitochondria, which is a crucial step in the apoptosis pathway [44]. Therefore, the increased expression of Bax induced by oxo berberine can intensify the cell’s response

to DNA damage or cellular stress. Oxo berberine also has an effect on the expression of the *MDM2* gene in the *p53* signaling pathway. *MDM2* is a key regulator of *p53* activity. When *MDM2* binds to *p53*, *p53* becomes inactive or degraded [45]. Therefore, the influence of oxo berberine on *MDM2* can enhance *p53* activity by inhibiting the interaction between *MDM2* and *p53*, which, in turn, can activate the cellular response to DNA damage or stress.

In conclusion, oxo berberine is the main chemical in AFRE (*Arcangelisia flava* root extract) that is also the most concentrated. It is an important part of pharmacological networks in many types of breast cancer, such as familial breast cancer, estrogen-negative breast cancer, estrogen-positive breast cancer, and *HER2*-negative breast cancer. Oxo berberine has been proven to target 84 genes that control cancer proliferation and apoptosis signaling pathways. Verification results in molecular docking have also confirmed that oxo berberine has a very strong affinity for the receptors *PI3KCA*, *TP53*, *BCL2*, *CDK1*, *EGFR*, and *MAPK14*, all of which play pivotal roles in regulating the cell cycle and apoptosis in breast cancer. *In vitro* experimental findings further support the previous analyses by demonstrating that oxo berberine compounds in AFRE can induce apoptosis and inhibit the cell cycle in *T47D* breast cancer cells. Overall, it has been revealed that oxo berberine in AFRE holds strong potential for breast cancer treatment; however, further *in vivo* research is needed to strengthen this scientific evidence.

Author Contribution Statement

Conception - RM, SS; Design - RM, AS; Supervision - RM, SS; Resources - SRZ; Material - RM, AS, AFF; Data Collection and/or Processing - RM, AS, AFF, SRZ; Analysis and/or Interpretation - RM, SS; Literature Search - RM, AS, AFF, SRZ; Writing - RM, AS, AFF, SRZ; Critical Review - RM, SS.

Acknowledgements

The authors express their gratitude to the Research and Community Service Institute (LP2M) of UIN Maulana Malik Ibrahim Malang, Ministry of Religious Affairs of the Republic of Indonesia, for their support, which enabled the research to be conducted effectively.

Funding Statement

This research was funded by the Research and Community Service Institute (LP2M) of UIN Maulana Malik Ibrahim Malang with grant number 615 Year 2024 under the National Applied Research scheme.

Approval

This study is part of a student's thesis that joins our research team.

Conflict of Interest

The authors declare that they have no conflict of interest

References

- Sung H, Ferlay J, Siegel RL, Laversanne M, Soerjomataram I, Jemal A, et al. Global Cancer Statistics 2020: GLOBOCAN Estimates of Incidence and Mortality Worldwide for 36 Cancers in 185 Countries. *CA Cancer J Clin.* 2021;71(3):209–49. <https://doi.org/10.3322/caac.21660>
- van den Boogaard WMC, Komninou DSJ, Vermeij WP. Chemotherapy Side-Effects: Not All DNA Damage Is Equal. *Cancers.* 2022;14(3):627. <https://doi.org/10.3390/cancers14030627>
- Luqmani YA. Mechanisms of Drug Resistance in Cancer Chemotherapy. *Med Princ Pract.* 2008;14(Suppl 1):35–48. <https://doi.org/10.1159/000086183>
- Coley HM. Mechanisms and strategies to overcome chemotherapy resistance in metastatic breast cancer. *Cancer Treat Rev.* 2008;34(4):378–90. <https://doi.org/10.1016/j.ctrv.2008.01.007>
- Mohamed A, Krajewski K, Cakar B, Ma CX. Targeted Therapy for Breast Cancer. *Am J Pathol.* 2013;183(4):1096–112. <https://doi.org/10.1016/j.ajpath.2013.07.005>
- Lovin ER, Arwati H, Ramadhani RB. *In vitro* intraerythrocytic antimalarial activity of akar kuning (*Arcangelisia flava* (L.) Merr.) stem aqueous extract in *Plasmodium falciparum*. *Folia Med Indones.* 2012;48(3):90.
- Maryani R, Monalisa SS, Rozik M. *In vitro* test of natural antibacterial activity of yellow-fruit moonseed *Arcangelisia flava* Merr. leaf on bacterium *Pseudomonas fluorescens* under different doses. *AACL Bioflux.* 2018;11(1):288–94.
- Maryani M, Rosdiana R. Peranan Imunostimulan Akar Kuning *Arcangelisia Flava* Merr Pada Gambaran Aktivasi Sistem Imun Ikan Mas (*Cyprinus carpio* L). *J Akuakultur Rawa Indones.* 2020;8(1):22–36.
- Keawpradub N, Dej-adisai S, Yuenyongsawad S. Antioxidant and cytotoxic activities of Thai medicinal plants named *Khaminkhruea*: *Arcangelisia flava*, *Coscinium blumeianum* and *Fibraurea tinctoria*. *Songklanakarin J Sci Technol.* 2005;27(Suppl 2):455–67.
- Cheng Q, Li F, Yan X, He J, Zhang H, Wang C, et al. Phytochemical and pharmacological studies on the genus *Arcangelisia*: A mini review. *Arab J Chem.* 2021;14(10):103346. <https://doi.org/10.1016/j.arabjc.2021.103346>
- Mutiah R, Kirana FO, Annisa R, Rahmawati A, Sandra F. Extract of yellow root (*Arcangelisia flava* (L.) Merr.) from several regions in Kalimantan: Alkaloid content and cytotoxicity towards widr colorectal cancer cells. *Indones J Cancer Chemoprevention.* 2020;11(2):84–9. <https://doi.org/10.14499/indonesianjcanchemoprev11iss2pp84-89>
- Wang X, Wang ZY, Zheng JH, Li S. TCM network pharmacology: A new trend towards combining computational, experimental and clinical approaches. *Chin J Nat Med.* 2021;19(1):1–11. [https://doi.org/10.1016/S1875-5364\(21\)60001-8](https://doi.org/10.1016/S1875-5364(21)60001-8)
- Lee AY, Park W, Kang TW, Cha MH, Chun JM. Network pharmacology-based prediction of active compounds and molecular targets in Yijin-Tang acting on hyperlipidaemia and atherosclerosis. *J Ethnopharmacol.* 2018;221:151–9. <https://doi.org/10.1016/j.jep.2018.04.027>
- Luo T ting, Lu Y, Yan S kai, Xiao X, Rong X lu, Guo J. Network Pharmacology in Research of Chinese Medicine Formula: Methodology, Application and Prospective. *Chin J Integr Med.* 2020;26(1):72–80. <https://doi.org/10.1007/s11655-019-3064-0>
- Mutiah R, Listiyana A, Suryadinata A, Annisa R, Hakim A, Anggraini W, et al. Activity of inhibit the cell cycle and induct apoptosis in HeLa cancer cell with combination

- of Sabrang onion (*Eleutherine palmifolia* (L.) Merr) and Starfruit Mistletoe (*Macrosolen cochinchinensis* (Lour.) Tiegh). *J Appl Pharm Sci*. 2018;8,(10):122–8. <https://doi.org/10.7324/JAPS.2018.81016>
16. Mutiah R, Bhagawan WS, Ma'arif B, Rahmandika JMS. Metabolite Fingerprinting *Eleutherine palmifolia* (L.) Merr. Using UPLC-QTOF-MS/MS. *Maj Obat Tradis*. 2019;24(3):139–59. <https://doi.org/10.22146/mot.44883>
 17. Stoner CL, Cleton A, Johnson K, Oh DM, Hallak H, Brodfuehrer J, et al. Integrated oral bioavailability projection using in vitro screening data as a selection tool in drug discovery. *Int J Pharm*. 2004;269(1):241–9. <https://doi.org/10.1016/j.ijpharm.2003.09.006>
 18. Jie LI, Shao-Ping W, Yu-Qi W, Lei SHI, Zhang ZK, Fan D, et al. Comparative metabolism study on chlorogenic acid, cryptochlorogenic acid and neochlorogenic acid using UHPLC-Q-TOF MS coupled with network pharmacology. *Chin J Nat Med*. 2021;19(3):212–24. [https://doi.org/10.1016/S1875-5364\(21\)60023-7](https://doi.org/10.1016/S1875-5364(21)60023-7)
 19. Lu H, Xie D, Qu B, Li M, He Y, Liu W. Emodin prevents renal ischemia-reperfusion injury via suppression of *p53*-mediated cell apoptosis based on network pharmacology. *Heliyon*. 2023;9(5):e15682. <https://doi.org/10.1016/j.heliyon.2023.e15682>
 20. Zhang R, Zhu X, Bai H, Ning K. Network Pharmacology Databases for Traditional Chinese Medicine: Review and Assessment. *Front Pharmacol*. 2019;10. <https://doi.org/10.3389/fphar.2019.00123>
 21. Hong L, Shi X, Zhao Y, Zhao G, Jiang H, Liu M, et al. Network pharmacology-guided and TCM theory-supported in vitro and in vivo component identification of Naoluoxintong. *Heliyon*. 2023;9(9):e19369. <https://doi.org/10.1016/j.heliyon.2023.e19369>
 22. Yang X, Tao Y, Xu R, Luo W, Lin T, Zhou F, et al. Analysis of active components and molecular mechanism of action of *Rubia cordifolia* L. in the treatment of nasopharyngeal carcinoma based on network pharmacology and experimental verification. *Heliyon*. 2023;9(6):e17078. <https://doi.org/10.1016/j.heliyon.2023.e17078>
 23. Zhang M, Zhang X, Pei J, Guo B, Zhang G, Li M, et al. Identification of phytochemical compounds of *Fagopyrum dibotrys* and their targets by metabolomics, network pharmacology and molecular docking studies. *Heliyon*. 2023;9(3):e14029. <https://doi.org/10.1016/j.heliyon.2023.e14029>
 24. Yu S, Kim T, Yoo KH, Kang K. The *T47D* cell line is an ideal experimental model to elucidate the progesterone-specific effects of a luminal A subtype of breast cancer. *Biochem Biophys Res Commun*. 2017;486(3):752–8. <https://doi.org/10.1016/j.bbrc.2017.03.114>
 25. Amalina ND, Salsabila IA, Zulfin UM, Jenie RI, Meiyanto E. *In vitro* synergistic effect of hesperidin and doxorubicin downregulates epithelial-mesenchymal transition in highly metastatic breast cancer cells. *J Egypt Natl Cancer Inst*. 2023;35(1):6. <https://doi.org/10.1186/s43046-023-00166-3>
 26. Moordiani M, Novitasari D, Susidarti RA, Ikawati M, Kato J ya, Meiyanto E. Curcumin Analogs PGV-1 and CCA-1.1 Induce Cell Cycle Arrest in Human Hepatocellular Carcinoma Cells with Overexpressed MYCN. *Indones Biomed J*. 2023;15(2):141–9. <https://doi.org/10.18585/inabj.v15i2.2147>
 27. Ye M, Liu J kai, Lu Z xin, Zhao Y, Liu S fang, Li L li, et al. Grifolin, a potential antitumor natural product from the mushroom *Albatrellus confluens*, inhibits tumor cell growth by inducing apoptosis in vitro. *FEBS Lett*. 2005;579(16):3437–43. <https://doi.org/10.1016/j.febslet.2005.05.013>
 28. Liu X, Wu J, Zhang D, Wang K, Duan X, Zhang X. A Network Pharmacology Approach to Uncover the Multiple Mechanisms of *Hedyotis diffusa* Willd. on Colorectal Cancer. *Evid Based Complement Alternat Med*. 2018;2018:e6517034. <https://doi.org/10.1155/2018/6517034>
 29. Florea AM, Büsselberg D. Cisplatin as an Anti-Tumor Drug: Cellular Mechanisms of Activity, Drug Resistance and Induced Side Effects. *Cancers*. 2011;3(1):1351–71. <https://doi.org/10.3390/cancers3011351>
 30. Hussain Y, Islam L, Khan H, Filosa R, Aschner M, Javed S. Curcumin–cisplatin chemotherapy: A novel strategy in promoting chemotherapy efficacy and reducing side effects. *Phytother Res*. 2021;35(12):6514–29. <https://doi.org/10.1002/ptr.7225>
 31. Kou Y, Li L, Li H, Tan Y, Li B, Wang K, et al. Berberine suppressed epithelial mesenchymal transition through cross-talk regulation of PI3K/AKT and RAR α /RAR β in melanoma cells. *Biochem Biophys Res Commun*. 2016;479(2):290–6. <https://doi.org/10.1016/j.bbrc.2016.09.061>
 32. Liu Z, Liu Q, Xu B, Wu J, Guo C, Zhu F, et al. Berberine induces *p53*-dependent cell cycle arrest and apoptosis of human osteosarcoma cells by inflicting DNA damage. *Mutat Res Mol Mech Mutagen*. 2009;662(1):75–83. <https://doi.org/10.1016/j.mrfmmm.2008.12.009>
 33. Wang J, Yang S, Cai X, Dong J, Chen Z, Wang R, et al. Berberine inhibits EGFR signaling and enhances the antitumor effects of EGFR inhibitors in gastric cancer. *Oncotarget*. 2016;7(46):76076–86. <https://doi.org/10.18632/oncotarget.12589>
 34. Li L, Wang X, Sharvan R, Gao J, Qu S. Berberine could inhibit thyroid carcinoma cells by inducing mitochondrial apoptosis, G0/G1 cell cycle arrest and suppressing migration via *PI3K-AKT* and *MAPK* signaling pathways. *Biomed Pharmacother*. 2017;95:1225–31. <https://doi.org/10.1016/j.biopha.2017.09.010>
 35. Mohammadlou M, Abdollahi M, Hemati M, Baharlou R, Doulabi EM, Pashaei M, et al. Apoptotic effect of berberine via Bcl-2, ROR1, and mir-21 in patients with B-CHRONIC lymphocytic leukemia. *Phytother Res*. 2021;35(4):2025–33. <https://doi.org/10.1002/ptr.6945>
 36. Thorburn A. Tumor Necrosis Factor-Related Apoptosis-Inducing Ligand (*TRAIL*) Pathway Signaling. *J Thorac Oncol*. 2007;2(6):461–5. <https://doi.org/10.1097/JTO.0b013e31805fea64>
 37. Tummers B, Green DR. Caspase-8: regulating life and death. *Immunol Rev*. 2017;277(1):76–89. <https://doi.org/10.1111/imr.12541>
 38. Yang K, Guo Y, Stacey WC, Harwalkar J, Fretthold J, Hitomi M, et al. Glycogen synthase kinase 3 has a limited role in cell cycle regulation of cyclin D1 levels. *BMC Cell Biol*. 2006;7(1):33. <https://doi.org/10.1186/1471-2121-7-33>
 39. Lee MH, Yang HY. Regulators of G1 cyclin–dependent kinases and cancers. *Cancer Metastasis Rev*. 2003;22(4):435–49. <https://doi.org/10.1023/A:1023785332315>
 40. Wijnen R, Pecoraro C, Carbone D, Fiuji H, Avan A, Peters GJ, et al. Cyclin Dependent Kinase-1 (CDK-1) Inhibition as a Novel Therapeutic Strategy against Pancreatic Ductal Adenocarcinoma (PDAC). *Cancers*. 2021;13(17):4389. <https://doi.org/10.3390/cancers13174389>
 41. Chang F, Lee JT, Navolanic PM, Steelman LS, Shelton JG, Blalock WL, et al. Involvement of PI3K/Akt pathway in cell cycle progression, apoptosis, and neoplastic transformation: a target for cancer chemotherapy. *Leukemia*. 2003;17(3):590–603. <https://doi.org/10.1038/sj.leu.2402824>
 42. Ali AK, Nandagopal N, Lee SH. IL-15–PI3K–AKT–mTOR: A Critical Pathway in the Life Journey of Natural Killer

- Cells. *Front Immunol.* 2015;6:355. <https://doi.org/10.3389/fimmu.2015.00355>
43. Campbell KJ, Tait SWG. Targeting BCL-2 regulated apoptosis in cancer. *Open Biol.* 2018;8(5):180002. <https://doi.org/10.1098/rsob.180002>
44. González de Aguilar JL, Gordon JW, René F, de Tapia M, Lutz-Bucher B, Gaiddon C, et al. Alteration of the Bcl-x/Bax Ratio in a Transgenic Mouse Model of Amyotrophic Lateral Sclerosis: Evidence for the Implication of the *p53* Signaling Pathway. *Neurobiol Dis.* 2000;7(4):406–15. <https://doi.org/10.1006/nbdi.2000.0295>
45. Azzahra SNA, Hanif N, Hermawan A. *MDM2* is a Potential Target Gene of Glycyrrhizic Acid for Circumventing Breast Cancer Resistance to Tamoxifen: Integrative Bioinformatics Analysis. *Asian Pac J Cancer Prev.* 2022;23(7):2341–50. <https://doi.org/10.31557/APJCP.2022.23.7.2341>



This work is licensed under a Creative Commons Attribution-Non Commercial 4.0 International License.